Neurochem Res (2008) 33:134–149
DOI 10.1007/s11064-007-9426-6

ORIGINAL PAPER

Umbilical Cord Blood Stem Cell Mediated Downregulation of Fas Improves Functional Recovery of Rats after Spinal Cord Injury

Venkata Ramesh Dasari · Daniel G. Spomar · Liang Li · Meena Gujrati · Jasti S. Rao · Dzung H. Dinh

Accepted: 22 June 2007 / Published online: 17 August 2007

Abstract Human umbilical cord blood stem cells (hUCB), due to their primitive nature and ability to develop into nonhematopoietic cells of various tissue lineages, represent a potentially useful source for cell-based therapies after spinal cord injury (SCI). To evaluate their therapeutic potential, hUCB were stereotactically transplanted into the injury epicenter, one week after SCI in rats. Our results show the presence of a substantial number of surviving hUCB in the injured spinal cord up to five weeks after transplantation. Three weeks after SCI, apoptotic cells were found especially in the dorsal white matter and gray matter, which are positive for both neuron and oligodendrocyte markers. Expression of Fas on both neurons and oligodendrocytes was efficiently downregulated by hUCB. This ultimately resulted in downregulation of caspase-3 extrinsic pathway proteins involving increased expression of FLIP, XIAP and inhibition of PARP cleavage. In hUCB-treated rats, the PI3K/Akt pathway was also involved in antiapoptotic actions. Further, structural integrity of the cytoskeletal proteins α-tubulin, MAP2A&2B and NF-200 has been preserved in hUCB treatments. The behavioral scores of hind limbs of hUCB-treated rats improved significantly than those of the injured group, showing functional recovery. Taken together, our results indicate that hUCB-mediated downregulation of Fas and caspases leads to functional recovery of hind limbs of rats after SCI.

Keywords Umbilical cord blood stem cells · Apoptosis · Fas · Caspase-3 · Spinal cord Injury · Functional recovery

Abbreviations

APC	Adenomatous polyposis coli
BBB	Basso Beattie Bresnahan locomotor scoring
BCA	Bicinchoninic acid
BDNF	Brain derived neurotrophic factor
bFGF	Basic fibroblast growth factor
CHAPS	3-[(3-Cholamidopropyl) dimethylammonio]-1-propanesulfonate
CNPase	2′,3′-Cyclicnucleotide-3′-phosphodiesterase
DAB	Diaminobenzidine
DAPI	4′,6-Diamidino-2-phenylindole dihydrochloride
DPI	Days post injury
DTT	Dithiothreitol
FBS	Fetal bovine serum
FITC	Fluorescein isothiocyanate
FLIP	FLICE-inhibitory protein
hEGF	Human epidermal growth factor
HRP	Horseradish peroxidase
hUCB	Human umbilical cord blood stem cells
MAP2A&2B	Microtubule associated protein 2A & 2B
MBP	Myelin Basic Protein
β-NGF	Beta-nerve growth factor
NF-200	Neurofilament H-200 kDa
NT-3	Neurotrophic hormone-3
PARP	Poly [ADP-ribose] polymerase

V. R. Dasari · L. Li · J. S. Rao
Department of Cancer Biology and Pharmacology, University of Illinois College of Medicine, Peoria, IL 61656, USA

D. G. Spomar · J. S. Rao · D. H. Dinh (✉)
Department of Neurosurgery, University of Illinois College of Medicine at Peoria, One Illini Drive, Peoria, IL 61605, USA
e-mail: ddinh@uic.edu

M. Gujrati
Department of Pathology, University of Illinois College of Medicine at Peoria, Peoria, IL 61656, USA

PBS	Phosphate buffered saline
PMSF	Phenyl methane sulfonyl fluoride
RA	Retinoic acid
SCI	Spinal cord injury
XIAP	X-linked inhibitor of apoptosis protein

Introduction

Potential therapies to improve functional recovery after traumatic spinal cord injury (SCI) are still not available. Spinal cord injury induced by trauma compresses and shears neuronal and glial cell types and their processes in the immediate vicinity of the impact. As a consequence, cells spill their intracellular contents into the extracellular matrix. This pathophysiological occurrence initiates a cascade of biochemical changes that results in necrotic and apoptotic cell death (1). Although cell death occurs within minutes in the grey matter of the injury epicenter, apoptotic death of oligodendroglia is apparent in distal white matter tracts several days post-injury. This delayed phase of oligodendroglial death may contribute to sensorimotor deficits through demyelination of intact neural pathways that survived the initial trauma. The phenomenon of secondary injury, which extends for days after the initial trauma, presents the first opportunity for intervention after SCI (2). Since the natural capacity of the central nervous system to recover from injury is limited, current SCI research focuses on the promotion of axonal growth and reduction of neuronal degeneration.

Apoptosis, regulated mainly by caspases (3), can be initiated by diverse stimuli, including extracellular signals acting at specific receptors such as CD95/Fas/APO1 and tumor necrosis factor (TNF) receptor (4). Early apoptosis of neural cells including neurons is followed by a delayed wave of predominantly oligodendroglial apoptosis in degenerating white matter tracts (5–9). Studies of apoptosis in white matter after dorsal cordotomy or after transection suggest that glial apoptosis occurs, at least in part, as a consequence of axonal degeneration (10, 11). Several studies have implicated the apoptotic role of caspases in the injured spinal cord (12–21). An increase in the number of cells expressing Fas was observed within 72 hours of SCI (22). Fas expression, activation of caspases 3 and 8, and apoptosis occur in a temporally similar fashion after SCI (23). Demjen et al. reported that FasL neutralizing antibodies improved neurological outcome after SCI (24). Fas deficiency on SCI in $FAS^{Lpr/lpr}$ mutant mice is associated with improved locomotor recovery, axonal sparing and preservation of oligodendrocytes and myelin (12). Hence, it is hypothesized that decreasing apoptosis in both oligodendrocytes and neurons by decreasing the expression of Fas may improve neurological outcome after SCI.

Human umbilical cord blood (hUCB) cells, due to their primitive nature and ability to develop into nonhematopoietic cells of various tissue lineages, including neural cells, may be useful as an alternative cell source for cell-based therapies requiring either the replacement of individual cell types and/or substitution of missing substances (25). Recently, hUCB progenitor cells were shown to possess significant advantages over bone marrow in terms of proliferative capacity and immunologic reactivity (26). Therefore, hUCB may be considered as an attractive source of hematopoietic stem cells for both research and clinical applications. Hence, in an attempt to understand the *in vivo* processes associated with the proposed hUCB therapeutic value, we designed the present study to evaluate neural cell differentiation of hUCB in the injured spinal cord of rat, to demonstrate the anti-apoptotic effects of hUCB after SCI, and to assess improvement in neurological functions after hUCB transplantation.

Materials and methods

Spinal cord injury of rat model

Moderate spinal cord injury was induced using the weight drop device (NYU Impactor) as reported previously (8, 15). Rats were assigned to different groups as described in Table 1. Briefly, adult male rats (Lewis; 250–300 g) were anesthetized with ketamine (100 mg/kg; ip) and xylazine (5 mg/kg; ip) (both from Med-Vet International, Mettawa, IL). A laminectomy was performed at the T9-T11 level exposing the cord beneath without disrupting the dura. The spinous processes of T8 and T12 were then clamped to stabilize the spine, and the exposed dorsal surface of the cord at T10 was subjected to a weight drop impact using a 10 g rod (2.5 mm in diameter) dropped at a height of 12.5 mm. After injury, the muscles and skin were closed in layers, and the rats were placed in a temperature and humidity-controlled chamber overnight. Cefazolin (25 mg/kg) (Fisher, Hanover Park, IL,) was given to prevent urinary tract infection for 3–7 days. Manual expression of the urinary bladder was performed two times per day until reflex bladder emptying was established. The Institutional Animal Care and Use Committee of the University of Illinois College of Medicine at Peoria approved all surgical interventions and post-operative animal care.

Behavioral assessment after SCI

BBB Scoring: A behavioral test was performed to measure the functional recovery of rats' hind limbs following the

Table 1 Experimental groups and number of animals used for each experiment

Group No.	Group Description	Designation	No. of animals studied	Immuno-histochemistry	Caspase-3 activity	Western Blot	Behavioral studies
1.	Control animals with laminectomy and PBS injected	Sham control	10 + 5*	4	3	3	10 + 5*
2.	Spinal cord injured and untreated animals	Injured	18 + 5*	7	5	6	18 + 5*
3.	Spinal cord injured and hUCB transplantation	hUCB treated	19 + 5*	7 + 5*	5	7	19 + 5*
4.	Spinal cord injured and cyclosporine treated	Cyclosporine treated	5*	-	-	-	5*

Three animals died unexpectedly during the course of the experiment; two from group 2(died of hematuria), one from group 3 (died of hematuria). Early data from these animals were omitted from the analysis. Animals were sacrificed after 21d after SCI (i.e., 14 d after transplantation of hUCB)

*Animals sacrificed after 6 weeks. In hUCB treated group 5 animals were used for immunohistochemistry studies on *in vivo* transdifferentiation of hUCB in the injured spinal cord after 5 weeks of grafting

procedure described in Basso et al. (27). The scale used for measuring hind limb function with these procedures ranges from a score of 0, indicating no spontaneous movement, to a maximum score of 21, with an increasing score indicating the use of individual joints, coordinated joint movement, coordinated limb movement, weight-bearing, and other functions. Rats were first gently adapted to the open field used for the test. After a rat had walked continuously in the open field, two investigators conducted 4-min testing sessions on each leg. Two individuals 'blinded' to rat treatment status performed the open-field test. Two BBB tests were performed at 1 and 2 days after injury, after transplantation of hUCB and the rats were subsequently tested weekly for 5 weeks. Behavioral outcomes and examples of specific BBB locomotor scores were recorded using digital video.

Narrow-beam crossing: This test evaluates the ability of the rats to balance on 30 cm elevated wooden beams with a length of 1 m. Different beam shapes were used to increase the level of difficulty: two beams with rectangular cross-sections (2 × 2 cm; 1.2 × 1.2 cm) and a beam with a round cross-section (2.5 cm in diameter) (28). Crossing one beam by properly placing both hindlimbs was scored as 2 points; a total of 1.5 points was assigned when an animal placed only one paw plantar on the beam. Only 1 point was given if the rat was able to cross the whole beam but was unable to place the hind paws, and 0.5 points was given if the rat could only traverse half of the beam. The score was zero in cases in which the rat was not able to cross at least half of the beam. The scores of all three beams were added to a maximum score of 6 points.

Contact placing response: Contact placing is elicited by lightly touching the skin of the dorsal side of the foot without joint displacement (29, 30). The animal responds by lifting the hind leg and placing it upon the obstacle. The animals were held, supported by the upper body, with the hindlimbs hanging free. The dorsum of each foot was touched with the edge of a piece of paper. The total number of placing responses of ten trials per limb was noted and the placing rate for individual animals was determined from baseline data taken as 100%.

Culture and *in vitro* differentiation of hUCB

Human umbilical cord blood was collected from healthy volunteers with informed consent and according to a protocol approved by the Institutional Review Board. Human umbilical cord blood was enriched by sequential Ficoll density gradient purification followed by selection of cells with $CD44^+$ markers. The nucleated cells were suspended at a concentration of 1×10^7/mL in Mesencult basal medium (Stem Cell Technologies, USA) supplemented with 20% FBS (Hyclone, Logan, UT) and 1% Penicillin-Streptomycin (Invitrogen, Carlsbad, CA) and plated in 100 mm culture dishes. The cells were incubated for 3 days and the nonadherent cells were removed with medium replacement. After the cultures reached confluency, the cells were lifted by incubation with 0.25% trypsin and 1 mM EDTA at 37°C for 3 to 4 min. They were diluted at a ratio of 1:2 or 1:3 and replated and cultured at 37°C in an incubator with a 5% CO_2 atmosphere. For *in vitro* differentiation, an acclimatization step was carried out 24 h prior to neural induction by replacing the growth medium with preinduction medium consisting of Neurobasal medium (Invitrogen, Carlsbad, CA) supplemented with 10% FBS (Hyclone, Logan, UT), 1% Penicillin-Streptomycin (Invitrogen, Carlsbad, CA), 1% 200 mM L-Glutamine (Mediatech Inc.-Fisher, Hanover Park, IL),

2% B27 (Invitrogen, Carlsbad, CA), 1% N2 (Invitrogen, Carlsbad, CA), bFGF (10 ng/mL, Invitrogen, Carlsbad, CA), β-NGF (10 ng/mL, Sigma, St. Louis, MO), BDNF (10 ng/mL, EMD Biosciences, San Diego, CA), and NT-3 (10 ng/mL, EMD Biosciences, San Diego, CA). Neural differentiation was then initiated the following day by incubating the cells in neurogenic medium [preinduction medium with 0.5 μM retinoic acid (Sigma, St. Louis, MO) and hEGF (10 ng/mL, Sigma, St. Louis, MO)]. The cells were then observed for differentiation from 6 to 10 days.

Intraspinal grafting of hUCB

BBB locomotor rating scores were obtained before transplantation of hUCB and every week after SCI. Animals were reanesthetized as described above, and the laminectomy site was re-exposed. Sham control group animals were injected 7 days after laminectomy with 5 μL of sterile PBS using a 10 μL Hamilton syringe. The hUCB-treated group was injected 7 days after SCI, with 5 μL mononuclear cell layer of hUCB (5×10^5 cells/μL) diluted in sterile PBS. These cells were delivered into the contusion site at a rate of 0.5 μL/min using a 10 μL Hamilton syringe. Thus, a total of 2.5×10^6 cells were grafted into each injured spinal cord. For the hUCB-transplanted group, Cyclosporine (10 mg/kg) (Bedford Labs, Bedford, OH) was administered as an immunosuppressant for 3 days after transplantation of hUCB. Cyclosporine-treated group rats received Cyclosporine (10 mg/kg) for 3 days after SCI.

Immunocytochemistry

Cultured hUCB were characterized with antibodies against neural and oligodendroglial markers. For this, cultured cells plated in 2-well chamber slides were rinsed twice with PBS, then fixed in 4% paraformaldehyde. After additional PBS rinses, cells were blocked with 0.1 M PBS with 1% BSA for 1 h. Primary antibodies specific for neurons and oligodendrocytes were used to label the plated cells. Primary antibodies (1:100 dilution) specific for hUCB [mouse anti-CD44 (Biomeda, Foster City, CA) or rabbit anti-CD44 (Abcam, Cambridge, MA)], for neurons [mouse anti-nestin (Chemicon, Temecula, CA), rabbit anti-NF200 (Chemicon, Temecula, CA)], for oligodendrocytes [(mouse anti-CNPase (Abcam, Cambridge, MA), mouse anti-O1 (R&D Systems, Minneapolis, MN] were diluted in 0.1 M PBS containing 1% BSA and applied overnight at 4°C. Appropriate fluorescence-tagged goat anti-mouse or anti-rabbit secondary antibodies were diluted 1:200 in 0.1 M PBS containing 1% BSA and applied individually for 1 to 2 h at room temperature. The cells were observed using a fluorescence microscope (Olympus IX71, Olympus, Melville, NY) and/or a confocal microscope (Olympus Fluoview, Olympus, Melville, NY) and photographed.

Immunohistochemistry

Animals were sacrificed at 3 weeks post injury for studies on apoptosis and 6 weeks post injury for studies on transdifferentiation of hUCB to neural phenotypes under *in vivo* conditions in the injured spinal cord. At specified times, rats were deeply anesthetized with ketamine/xylazine and intracardially perfused with 4% paraformaldehyde in 0.1 M phosphate buffer (pH 7.4). The spinal cord was removed and fixed for 2 h. Serial sections (5 μm) were made from spinal cord centered on the injury epicenter. Representative sections were stained with hematoxylin and eosin and Luxol fast blue to assess tissue morphology and determine the injury epicenter. Serial sections (1 section every 200 μm) obtained from 1 and 2 mm of tissue rostral and caudal to the epicenter were used for immunohistochemical analysis of apoptosis by *in situ* TUNEL or activated caspase-3-mediated apoptotic proteins. For *in vivo* differentiation, neuronal or glial markers were detected using fluorescent staining. We used the following primary antibodies: mouse anti-CD44 (Biomeda, Foster City, CA) or rabbit anti-CD44 (Abcam, Cambridge, MA), rabbit anti-NF200 (Chemicon, Temecula, CA), mouse anti-βIII-Tubulin (Chemicon, Temecula, CA), mouse anti-APC (EMD Biosciences, San Diego, CA), mouse anti-myelin basic protein (BD Biosciences, Franklin Lakes, NJ). Rabbit anti-Caspase-3 (Cell Signaling Technology Inc., Beverly, MA) was used for immunostaining of caspases. For immunostaining of cytoskeletal proteins, mouse anti-α-tubulin (EMD Biosciences, San Diego, CA), rabbit anti-neurofilament H 200 kDa (NF200) (Chemicon, Temecula, CA) and mouse anti-MAP-2A&2B (Chemicon, Temecula, CA) were used. After staining with primary antibodies (1:100 dilution), the sections were washed three times in PBS (10 min/wash) and incubated in goat anti-mouse or anti-rabbit HRP-conjugated secondary antibodies (1:200 dilution). For immunofluorescence studies, the sections were washed three times in PBS (10 min/wash) and incubated in Texas Red conjugated anti-mouse secondary antibody or FITC-conjugated anti-rabbit secondary antibody (all at 1:200 dilution) for 1 h at room temperature. Sections were then washed three times in PBS (10 min/wash), counter stained with DAPI or Hoechst 33343 and cover slipped using fluorescent mounting medium (Dako, Carpinteria, CA), and observed using both fluorescence microscope (Olympus IX71, Olympus, Melville, NY) and/or confocal microscope (Olympus Fluoview, Olympus, Melville, NY). Negative controls (without primary antibody or using isotype specific IgG) were maintained for all the samples. Sections in which polymerase was omitted were used as negative control (for TUNEL). A neuropathologist, who was blinded to the treatment group and study, evaluated the sections.

Cell counting

All morphological analyses were performed with tissue identified by animal number. Sections representing 1 and 2 mm of tissue from the injury epicenter of animals at 21 DPI and controls were used to quantify immunoreactive cells. Cell counting was carried out in 10 sections (5 rostral and 5 caudal to the injury epicenter) per segment per animal in a 1 mm^2 area of the dorsal white matter and dorsal grey matter using Image-Pro Discovery software (Media Cybernetics, Silver Spring, MD). Apoptotic cells in the white and grey matter regions were counted in three randomly chosen sections per 1 mm length of spinal cord, and the numbers were averaged. These regions were chosen because of the spared tissue even after SCI.

Immuno blot analysis

Different protein levels in spinal cord tissue at 3 weeks after SCI were compared with those in laminectomy controls and treated samples. For immuno blot analysis, rats were euthanized, and 5 mm lengths of spinal cord centered on T10 (the injury site) were rapidly removed, weighed, and frozen at –70°C until necessary for further experimentation. The tissues were resuspended in 0.2 mL of homogenization buffer pH 7.4 [250 mM sucrose, 10 mM HEPES, 10 mM Tris-HCl, 10 mM KCl, 1% NP-40, 1 mM NaF, 1 mM Na_3VO_4, 1 mM EDTA, 1 mM DTT, 0.5 mM PMSF plus protease inhibitors: 1 μg/mL pepstatin, 10 μg /mL leupeptin and 10 μg/mL aprotinin] and homogenized in a Dounce homogenizer. Tissue homogenate was centrifuged at 20,000 × *g* for 15 min at 4°C and the protein levels in the supernatant were determined using the BCA assay (Pierce, Rockford, IL). Samples (40 μg of total protein per well) were subjected to 10%–14% SDS-PAGE and transferred onto nitrocellulose membranes, and the reaction was detected with Hyperfilm-MP autoradiography film (Amersham, Piscataway, NJ). For Western blot analysis, the following antibodies were used: rabbit anti-NF200 (1:500; Chemicon, Temecula, CA), mouse anti-CNPase (1:500; Abcam, Cambridge, MA), mouse anti-Fas (1:5000; BD Biosciences, Franklin Lakes, NJ), rabbit anti-FasL (1:500; Abcam, Cambridge, MA), rabbit anti-FADD (1:200; Santa Cruz Biotechnology, Santa Cruz, CA), rabbit anti-Caspase 8 (1:500; Biovision, Mountain View, CA), rabbit anti-Caspase-3 (1:1000; Cell Signaling Technology Inc., Beverly, MA), rabbit anti-Caspase 10 (1:1000; Cell Signaling Technology Inc., Beverly, MA), rabbit anti-PARP (1:1000; Cell Signaling Technology Inc., Beverly, MA), rabbit anti-XIAP (1:1000; Cell Signaling Technology Inc., Beverly, MA), rabbit anti-FLIP (1:1000; Cell Signaling Technology Inc., Beverly, MA), rabbit anti-AIF (1:1000; Cell Signaling Technology Inc., Beverly, MA), rabbit anti-BCL-2 (1:500; Santa Cruz Biotechnology, Santa Cruz, CA), rabbit anti-AKT (1:1000; Cell Signaling Technology Inc., Beverly, MA), mouse anti-phospho-AKT (1:1000; Cell Signaling Technology Inc., Beverly, MA), mouse anti-PI3 Kinase (1:5000; BD Biosciences, Franklin Lakes, NJ) and mouse anti-GAPDH (1:1000; Novus Biologicals, Littleton, CO). The membranes were blocked with 5% nonfat skim milk in TBS for 1 h at room temperature and then incubated with primary antibodies overnight at 4°C. The membranes were then processed with HRP-conjugated secondary antibodies. Immunoreactive bands were visualized using chemiluminescence ECL Western blotting detection reagents (Amersham, Piscataway, NJ). Experiments were performed in triplicate to ensure reproducibility. Values for injured, treated and control samples ($n \geq 3$ each group) were compared using one-way ANOVA test. A p value of <0.05 was considered significant.

In situ terminal-deoxy-transferase mediated dUTP nick end labeling (TUNEL) assay

A TUNEL apoptosis detection kit (Upstate Biotechnology Inc, Lake Placid, NY) was used for DNA fragmentation fluorescence staining according to the manufacturer's protocol. Briefly, injured, hUCB-treated and sham control rats ($n \geq 4$) were perfusion-fixed with 4% paraformaldehyde in 0.1 M phosphate buffer (pH 7.4). Serial 5 μm spinal cord sections at 200 μm intervals were stained with hematoxylin, eosin and Luxol Fast Blue to identify the injury epicenter. Tissue sections at the injury epicenter and at 1000 μm, 1500 μm and 2000 μm rostral and caudal were incubated with a reaction mix containing biotin-dUTP and terminal deoxynucleotidyl transferase for 60 min. Fluorescein-conjugated avidin was applied to the sample, which was then incubated in the dark for 30 min. Positively stained fluorescein-labeled cells were visualized and photographed by fluorescence microscopy.

Determination of caspase-3 activity

Caspase-3 activity of tissue samples was measured using Caspase-3 assay kit (Sigma, St. Louis, MO). The Caspase-3 colorimetric assay is based on the hydrolysis of acetyl-Asp-Glu-Val-Asp p-nitroanilide (Ac-DEVD-pNA) by caspase-3, resulting in the release of the p-nitroaniline (pNA) moiety. p-Nitroaniline is detected at 405 nm ($\varepsilon_{mM} = 10.5$). The concentration of the pNA released from the substrate is calculated from either the absorbance values at 405 nm or from a calibration curve prepared with pNA standards. Tissue between 1 and 2 mm from the injury epicenter were homogenized in 1X lysis buffer (250 mM HEPES, pH 7.4, 25 mM CHAPS, 25 mM DTT). Tissue homogenates were centrifuged at 20,000 × g for 15 minutes at 4°C in a microcentrifuge, and the supernatant was used for the measurement of caspase-3 activity using the 96-well plate

micro assay method. In a final volume of 100 µl supernatant (= 50 µg), each test sample was incubated for 30 min. at room temperature in the working solution containing synthetic caspase-3 substrate, Ac-DEVD-AMC. The absorbance was read at 405 nm in an ELISA plate reader for a period of 30 min. Ac-DEVD-CHO inhibitor is used for inhibitor studies. Caspase-3 activity was calculated using a *p*-nitroaniline calibration curve, as micromolar per gram of wet tissue. The data is plotted as A_{405} versus time for each sample and activity is calculated as pmol/min.

Statistical analyses

Quantitative data from cell counts, immuno blot analysis, Caspase-3 activity assay and locomotor behavior scores were evaluated for statistical significance by one-way ANOVA with replications. Data for each group were represented as mean ± SEM and compared with other groups for significance by one-way Analysis of Variance (ANOVA) followed by Bonferroni's post hoc test (multiple comparison tests) using a statistical software package—Graph Pad Prism version 3.02. Results were considered statistically significant at $p < 0.05$ and $p < 0.01$.

Results

Trans-differentiation of hUCB to neural phenotypes

The capability of hUCB to differentiate into neural phenotypes before and after intraspinal grafting was assessed using double labeling immunofluorescence technique. When exposed to hEGF/RA in neurogenic medium, hUCB morphologically appear to take on some of the features of neural cells in culture, such as long bipolar extensions and branching ends. After neural culture, cells from hUCB expressed the neural antigens found in neurons (stained by Nestin and NF200) and oligodendrocytes (stained by CNPase and O1) (Fig. 1A). Neural differentiation was observed after 7 days in culture for hUCB (Figs. 1C and 1D). After differentiation, these cells were maintained up to 30 days to avoid any artifacts. About 65–70% of hUCB showed trans-differentiation to neural phenotypes. These results were further confirmed by western blot analysis using both undifferentiated and differentiated hUCB (Fig. 1E). For comparison of neural proteins, we used rat whole brain extract as positive control. Differentiated hUCB show significant amounts of NF-200 (neural marker) and CNPase (oligodendrocyte marker), as confirmed by quantitative analysis (Fig. 1F). Out of total differentiated population of hUCB, cells expressing neural marker, NF-200 constituted the major proportion (48.36%) followed by oligodendrocyte marker, CNPase (31.79%) and the remaining fraction other glial markers (data not shown). The hUCB expressed these markers only after culture in the neurogenic differentiation media. Next, we addressed whether the grafted hUCB would be able to survive and differentiate *in vivo* in the injured spinal cord. Two weeks after transplantation, robust survival of transplanted hUCB was observed in the spinal cords of hUCB-treated rats, with cells distributed around the cavities throughout the injury site. The transplanted cells migrated up to 2 mm rostrocaudally in the white matter and gray matter. These hUCB survived up to five weeks after transplantation in the injured spinal cord. Surviving hUCB labeled with antibodies against markers specific for hUCB (CD44) could be visualized. In treated rats, co-localization of hUCB with neurons (stained by βIII-tubulin and NF-200) and oligodendrocytes (stained by mature oligodendrocytic marker APC and MBP) (Fig. 1B) significantly establishes the differentiation of hUCB to specific neural phenotypes in the injured spinal cord. Out of the total differentiated hUCB *in vivo*, most surviving hUCB were oligodendrocytes (49.90%) followed by neurons (32.22%) present in the middle of the cord. These findings suggest that our transplantation strategies promote preferential survival and/or differentiation of hUCB toward oligodendrocyte and neural lineages. In hUCB treated group, these hUCB differentiated neurons and oligodendrocytes were mostly observed in the dorsal region of the injury epicenter, up to 2 mm rostrocaudally. The highest density of hUCB was at the area of primary injury, and was gradually reduced as the border with intact spinal cord tissue was approached. No hUCB cells were found in areas of intact spinal cord. No similarly fluorescent cells were found in SCI only animals (injured group).

Apoptosis of cells following SCI is reduced by hUCB

We hypothesized that in order to have therapeutic potential and restore neurological functions, hUCB must reduce secondary processes within a few weeks. As a prelude to investigations on Fas-dependent caspase-3 activation, we first confirmed the occurrence of apoptosis in the spinal cord after SCI using nuclear staining by Hoechst 33343 and the TUNEL method (Fig. 2). Since we observed the differentiation of hUCB up to 2 mm of the injury epicenter, we confined our study to this region rostrocaudally. Nuclear staining with Hoechst 33343 identified the presence of apoptotic cells in the injured spinal cord tissue (Figs. 2A and 2B). In SCI rats, the number of apoptotic cells increased up to 42.38 ± 2, per mm^2 section regardless of whether the section was at 1 or 2 mm rostral or caudal to T10, within the dorsal region, especially around the lesion epicenter. Notably, we observed significant reduction in the

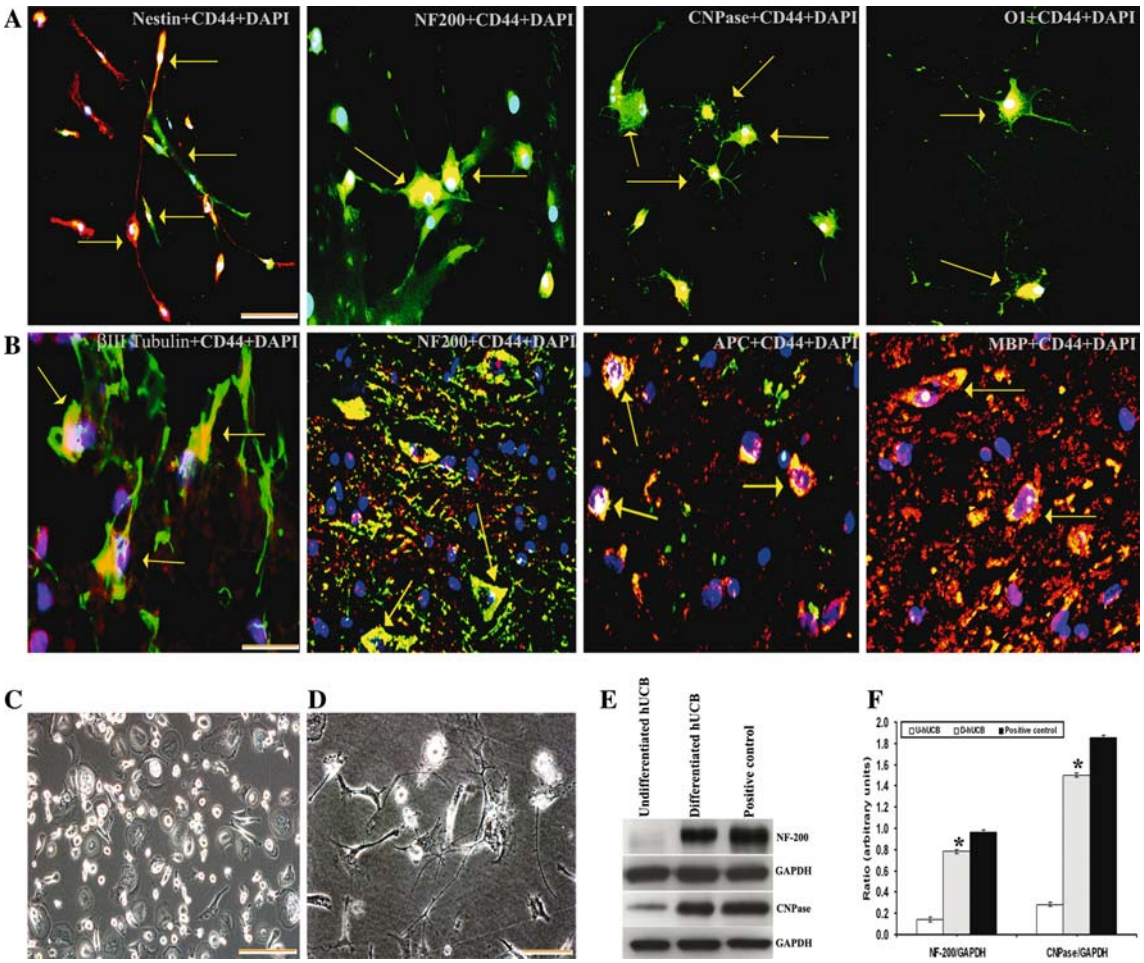

Fig. 1 Trans-differentiation of hUCB into neural phenotypes. (**A**) Photomicrographs of hUCB in mixed culture demonstrating neural proteins expressed by the cells before transplantation. FITC-conjugated- Nestin and NF-200 (for neurons) with Texas-red conjugated- CD44 (for hUCB); Texas-red conjugated –CNPase and O1 (for oligodendrocytes) with FITC-conjugated- CD44 (for hUCB). Cells displaying neuron like morphology with long axonal projections, CNPase-immunoreactive cells displaying morphology characteristic of oligodendrocytes, with flat cell body and short or long branched projections. (**B**) Confocal immunohistochemistry on longitudinal sections of the injured spinal cords of rats 5 weeks after transplantation is shown. Immunofluorescence analysis of cryosections indicates co-localization (yellow) of FITC-conjugated –βIII tubulin and NF-200 (for neurons) with Texas-red conjugated- CD44 (for hUCB); FITC conjugated-CD44 (for hUCB) with Texas-red conjugated -APC and -MBP (for oligodendrocytes) as shown by (↑). The results are from 3 independent sections between 1 and 2 mm from the injury epicenter from treated rats (n = 5). Bar = 100 μm. (**C**) Phase-contrast image of undifferentiated hUCB. (**D**) Phase-contrast image of differentiating hUCB after 4 days showing mixed population of differentiated neural phenotypes. (**E**) Western blot showing neural proteins in differentiated population. Equal amounts of protein (40 μg) were loaded onto 10%–14% gels and transferred onto nylon membranes, which were then probed with respective antibodies. The blots were stripped and reprobed with GAPDH to assess protein levels. (**F**) Quantitative estimation of neural proteins in Fig. F. (U-hUCB = Undifferentiated hUCB; D- hUCB = Differentiated hUCB; Positive control = Whole brain extract of rat). Results are from 3 parallel experiments from 3 separate cord blood preparations. A subpopulation of hUCB-derived cells growing in a monolayer before differentiation was found to be negative for all investigated antigens. Merged figures include colocalized markers, shown by (↑). For panels A, B and C, Bar = 100 μm. For panel D, Bar = 200 μm. (Error bars indicate SEM. * Significant at $p < 0.05$)

number of apoptotic cells in hUCB-treated sections (9 ± 1) (Fig. 2B). Spinal cord sections from injured and treated groups were analyzed for TUNEL-positive cells (Figs. 2A and 2B). In the injured rats, there was an increase in TUNEL-positive cells to an average of 34.89 ± 1 within the dorsal white matter, especially around the lesion epicenter, accompanied by tissue loss. However, in hUCB-treated sections TUNEL positive cells showed significant reduction (6.55 ± 1).

Subsequently, we focused the analysis of TUNEL positive cells in a 1 mm^2 area of the sections taken at 1 and 2 mm rostrocaudal to the epicenter. After 21 days SCI, injured spinal cord tissues showed higher numbers of TUNEL-positive cells in the vicinity of 1 and 2 mm from

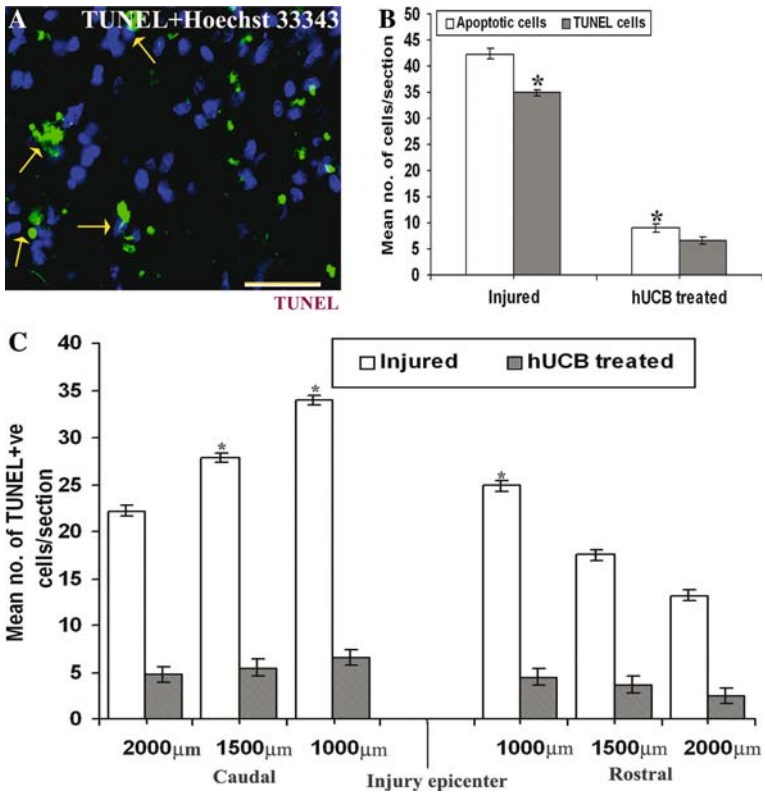

Fig. 2 Expression of apoptotic and TUNEL cells in spinal cord sections of rats. (**A**) Cryosections from injured rats after 3 weeks stained with Hoechst 33343 shows merged image showing TUNEL cells on apoptotic cells (↑). Bar = 100 μm. (**B**) Quantitative estimation of apoptotic and TUNEL cells. (Error bars indicate SEM. * Significant at $p < 0.05$). (**C**) Quantitative estimation of TUNEL-positive cells in the tissue sections up to 2 mm rostral and caudal to the injury epicenter. (Error bars indicate SEM. * Significant at $p < 0.05$). Results are from 3 independent sections between 1 and 2 mm from the injury epicenter ($n \geq 3$)

the injury epicenter, which upon treatment with hUCB decreased significantly (Fig. 2C). When compared to rostral region, caudal region showed higher numbers of TUNEL-positive cells. Similarly, higher numbers of TUNEL-positive cells were observed in the dorsal surface as compared to lateral surface. Based on these results, we confined our study to the dorsal surface of caudal region to the injury epicenter.

Down regulation of Fas expression by hUCB

Since the number of apoptotic cells and TUNEL positive cells are minimized in hUCB treatments, we decided to examine whether hUCB would decrease Fas levels in the treated rats. Co-localization studies with TUNEL and Fas on injured sections showed the presence of Fas on TUNEL cells indicating that these apoptotic cells undergo Fas-mediated apoptosis (Fig. 3A). Quantitative estimation shows the incidence of Fas on TUNEL-positive cells more in case of SCI rats (24 ± 1), which is significantly decreased in hUCB-treated (4 ± 1) group (Fig. 3B). In both sham control and hUCB-treated rats, Fas immunoreactivity was barely detectable in both white and grey matters. Fas immunoreactivity was easily detected in SCI rats, mainly in the neurons and oligodendrocytes. The number of Fas-positive cells in both white matter and grey matters were then determined in sections 2 mm caudal to the injury epicenter. Furthermore, double labeling immunohistochemistry with Fas and cell markers demonstrated that Fas is expressed both on neurons (Fig. 3C) and oligodendrocytes (Fig. 3E) of the spinal cord. Expression of Fas on apoptotic oligodendrocytes is more (44.48%) when compared to apoptotic neurons (38.01%) in SCI rats (Figs. 3D and 3F). In contrast, in hUCB treated groups Fas expression was reduced to significant levels in both neurons and oligodendrocytes.

Further, to understand the molecular mechanisms of hUCB downregulation of Fas, we analyzed the tissue lysates by Western blotting for the expression of Fas and its associated death ligands. Binding of FasL to its receptor Fas triggers the formation of a death inducing signaling complex (DISC) involving the recruitment of the adaptor protein FADD and caspase-8, which initiates a cascade of events leading to apoptotic cell death. Increase in the death ligands FasL, Fas and FADD were observed in the injured tissues as compared to hUCB treated tissues (Figs. 4A and 4B). These results confirm that SCI induces expression of Fas, which is downregulated by hUCB.

Inhibition of caspase-3 activated extrinsic pathway by hUCB

Next, caspase-3-mediated apoptotic pathway proteins were analyzed by Western blot analysis (Fig. 5). The activation of death ligands in the injured tissues triggered the activation of caspases-8, -10 and -3, which were efficiently downregulated by hUCB (Figs. 5A and 5B). Further,

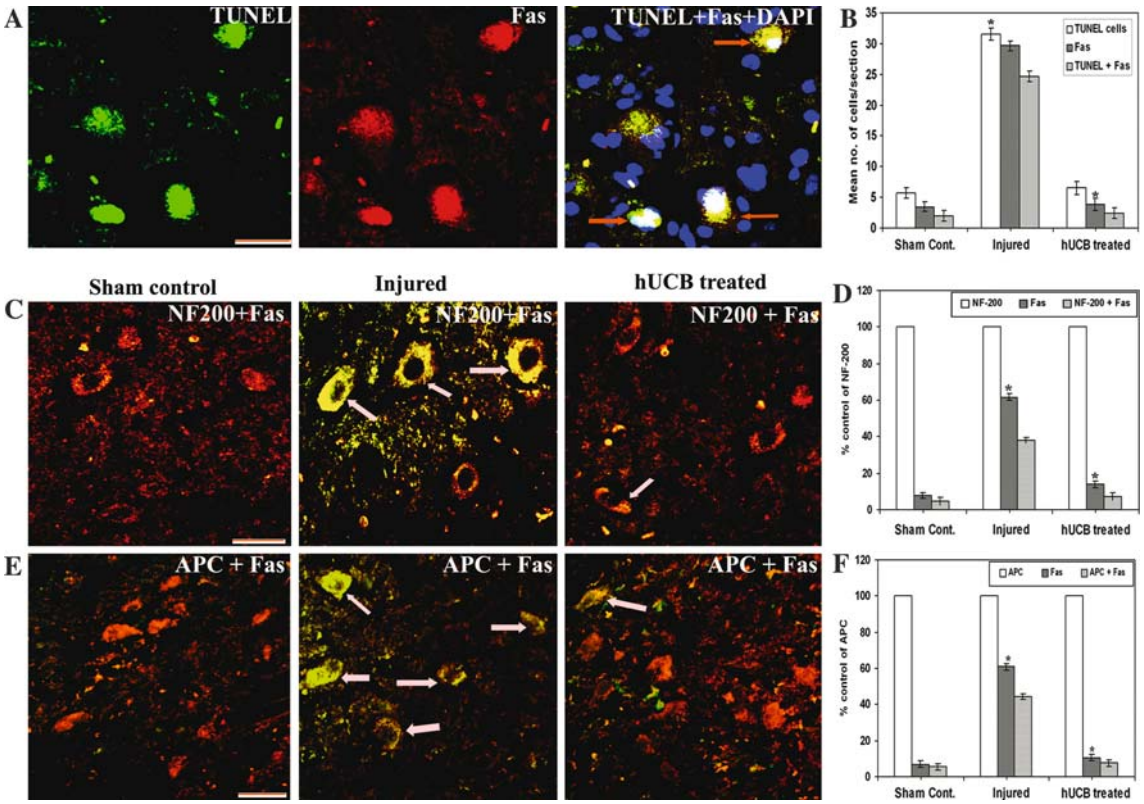

Fig. 3 Fas immunoreactivity on TUNEL positive cells. (**A**) Expression of Fas (Texas-red conjugated) on TUNEL positive cells (green) from injured sections. (**B**) Quantitative estimation of TUNEL, Fas and TUNEL + Fas cells in injured and treated groups. (**C**) Cryo-sections showing Co-localization of Fas and NF-200 (specific for neurons) and (**E**) Fas and APC (mature marker for oligodendrocytes) established the expression of Fas on neurons and oligodendrocytes (↑) undergoing apoptosis. Fas is FITC-conjugated and NF-200 and APC are Texas-red conjugated. Note a significant decrease in the expression of Fas in hUCB-treated sections. For panels A, C and E Bar = 100 μm. (**D**) Quantification of NF-200 + Fas cells and (**F**) APC + Fas cells. (Error bars indicate SEM. * Significant at $p < 0.05$). A total of more than 100 cells were counted per each field and more than five fields were chosen at random on each section. Results are from three sections between 1 and 2 mm caudal to the injury epicenter after 3 weeks SCI ($n \geq 3$)

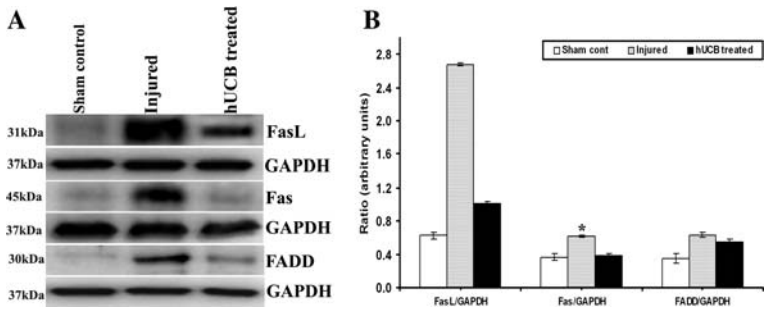

Fig. 4 Immunoblot analysis of Fas and other death ligands in spinal cord sections. Equal amounts of protein (40 μg) were loaded onto 10%–14% gels and transferred onto nylon membranes, which were then probed with respective antibodies. The blots were stripped and reprobed with GAPDH to assess protein levels. A shows the FasL, Fas and FADD proteins with respect to GAPDH; B shows their quantitative estimations. Inhibition of the apoptotic pathway by hUCB shows downregulation of FasL, Fas and FADD. Each blot is representative of experiments performed in duplicate with each sample ($n \geq 3$). Error bars indicate SEM. * Significant at $p < 0.05$

activity of caspase-3 enzyme in the tissues shows higher activity in the injured lysates compared to hUCB-treated tissues (Fig. 5C). In hUCB-treated rats, this activity is almost comparable to that of sham control uninjured rats, which confirms that some repair mechanisms are implicated by the hUCB. In order to demonstrate the type of neuronal cells participating in the process of apoptosis, co-localization experiments were performed using caspase-3

with NF-200 and APC antibodies. Caspase-3 expression was found in both neurons and oligodendrocytes (Fig. 6). The presence of higher number of caspase-3-positive neurons (Fig. 6A) and oligodendrocytes (Fig. 6B) in injured sections establishes the role of caspase-3 on apoptosis of oligodendrocytes and neurons after SCI, which showed a decreasing trend in hUCB-treated sections. Quantitation of the number of caspase-3-positive neurons and oligodendrocytes (Fig. 6C) indicated that oligodendrocytes comprise a major population of the cells that undergo caspase-3 mediated apoptosis. However, in hUCB treatments, there was significant reduction in the number of caspase-3 positive cells. Twenty-one days after injury, caspase-3-positive cells were observed at both 1 and 2 mm regions, supporting previous results that SCI activates a caspase-3-dependent apoptotic pathway in glial cells (13, 19).

Neuroprotective effects of hUCB

In order to understand the neuroprotective effects implemented by hUCB, we analyzed the inhibitor proteins of apoptotic pathway. In hUCB treatments upregulation of FLIP and XIAP was observed (Figs. 7A and 7B); these proteins are believed to serve as checkpoints of the apoptotic pathway in the cytosol. At the nuclear level, hUCB inhibited the cleavage of PARP. These data provide strong evidence that Fas and caspase-3 are implicated in the apoptotic cascade after SCI, and that hUCB probably inhibit apoptosis either by increasing the expression of FLIP and XIAP at the cytosolic level or by inhibiting the breakdown of PARP at the level of nucleus. Also, the inducer of apoptosis AIF was downregulated in hUCB treatments, with an upregulation of anti-apoptotic protein BCl2 (Figs. 7C and 7D). This ultimately resulted in the upregulation of survival pathway proteins Akt and PI3K in treated rats (Figs. 7E and 7F). Especially, the upregulation of phospho-Akt (Ser 473) in hUCB treatments indicates that hUCB are involved in phosphorylation of Akt at Ser 473 position, thereby activating the survival signaling PI3K/Akt pathway. Taken together, increase in Fas and caspase-3 and related apoptotic pathway proteins' expression, caspase-3 enzymatic assay results, and the nicking of chromatin support the occurrence of Fas-triggered caspase-3 activated apoptosis after traumatic SCI, which was efficiently downregulated by hUCB treatments.

Repair and maintenance of the structural integrity of the injured spinal cord by hUCB

The ability of hUCB to reduce Fas and activated caspase-3 in the dorsal white matter and gray matter prompted us to examine whether these hUCB help repair the structural integrity of the spinal cord at the injury epicenter. Sections from 21 days post SCI representing 1 and 2 mm segments rostral and caudal to the injury epicenter were analyzed for NF-200, MAP-2A&2B and α -tubulin. The preservation of the structural integrity of the neurons is indicated by the colocalization studies. Degradation of α-tubulin (Fig. 8A), MAP2A&2B (Fig. 8B) and NF200 (Fig. 8C) is seen in injured animals, which is improved with hUCB treatments. Analysis of cross-sectional area stained shows greater preservation of these proteins in hUCB treatments (Fig. 8 D). Our data suggests that downregulation of Fas and caspases by hUCB influences preservation of neuronal elements after injury in the spinal cord. Another possibility is that hUCB could differentiate into these proteins, thereby preserving cytoskeletal integrity of the injured spinal cord.

Recovery of locomotor function by hUCB

Finally, we tested whether inhibition of apoptotic pathway proteins and histopathological improvements induced by hUCB can be correlated with the functional recovery of rats. In the present study, we maintained cyclosporine-treated group as another control to check the potential of hUCB in promoting functional recovery in SCI rats. The effect of hUCB on recovery of locomotor function after SCI was evaluated according to 21-point locomotor BBB scale, which is widely used (27). All injured rats receiving the experimental treatments exhibited a severe locomotion deficit one day after surgery (Fig. 9A). The mean BBB score in the injured group was 5.75 ± 0.2 compared to 5.15 ± 0.5 in the hUCB-treated group before transplantation (7 days after SCI). A gradual recovery of hindlimb locomotion was seen over the following 2–3 weeks in all rats. Recovery of function improved slowly but steadily over the course of the five-week observation period in hUCB-treated and cyclosporine-treated groups. Rats in the transplanted groups showed a significant improvement in the BBB scale relative to the injured and cyclosporine-treated groups. For instance, after 14 days post-transplantation, some hUCB-treated rats were able to support their weight on the dorsal part of the paws while stationary or stepping, and others exhibited frequent to consistent steps with or without coordination. In contrast, injured rats only displayed movement of all three joints with occasional plantar placement. Overall, BBB scores were significantly improved at weeks 5 and 6 compared with week 1 after injury in hUCB-treated group ($p < 0.01$). Our analysis showed that hUCB-transplanted animals had a mean hindlimb score of 17.12 ± 0.36 at 5 weeks after transplantation, whereas in the injured and cyclosporine-treated groups, animals scored 12.04 ± 0.41 and 14.21 ± 0.29 after 6 weeks post-injury, respectively. Our results further indicate that the improved recovery of function in the transplanted group was exclusive to the beneficial effects

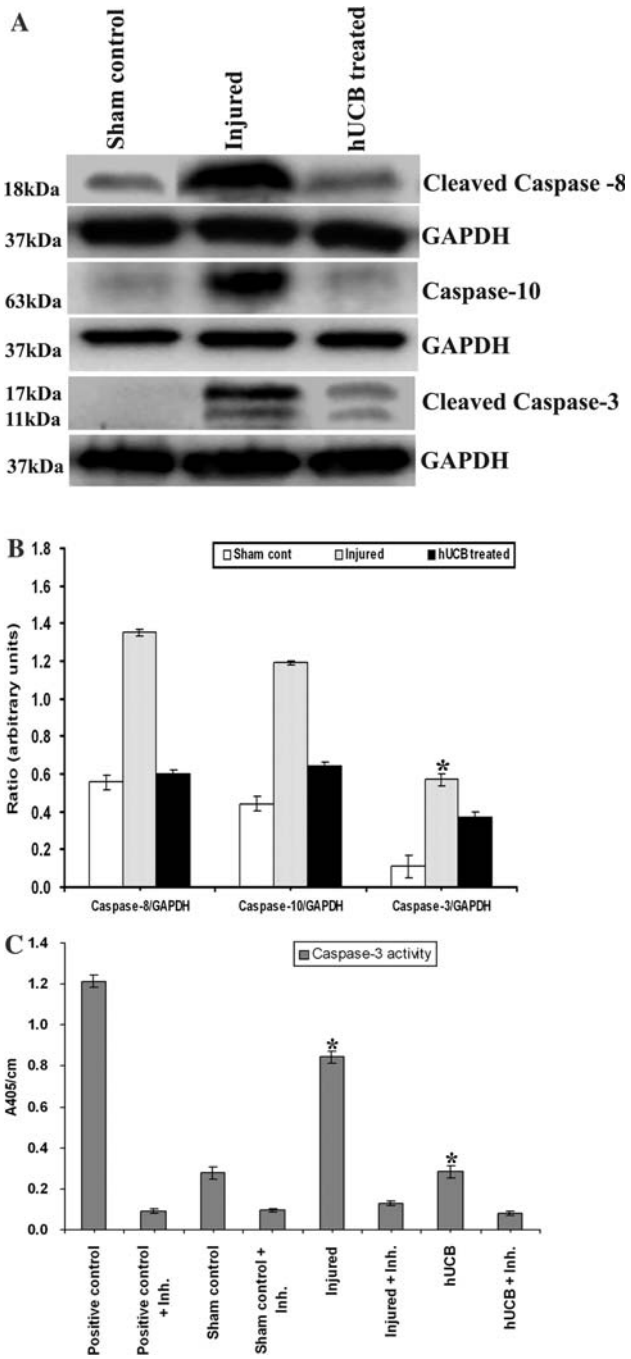

◀**Fig. 5** Activity of caspases after spinal cord injury. Equal amounts of protein (40 μg) were loaded onto 10%–14% gels and transferred onto nylon membranes, which were then probed with respective antibodies. The blots were stripped and reprobed with GAPDH to assess protein levels. (**A**) shows the caspase-3 mediated apoptotic pathway proteins with respect to GAPDH; (**B**) their quantitative estimation. Antisera for caspase-8 and caspase-3 recognize cleaved fragments also. Each blot is representative of experiments performed in duplicate with each sample ($n \geq 3$). Error bars indicate SEM. * Significant at $p < 0.05$. (**C**) Caspase-3 enzyme activity was assayed in tissue lysates of spinal cord. Equal amounts of protein (50 μg) were assayed for caspase-3 activity for 30 min in an ELISA plate reader, measuring absorption at 405 nm. Purified caspase-3 enzyme was used as a positive control. The injured tissues show maximum caspase-3 activity when compared to the treated tissues, which show activity similar to that of the control groups. Inh. = Ac-DEVD-CHO inhibitor. (Error bars indicate SEM. * Significant at $p < 0.05$). The experiment is repeated twice with triplicates ($n \geq 3$)

of hUCB transplantation, because there was no significant difference in the performance of the injured and cyclosporine-treated groups.

Narrow-beam crossing

This test reflects the capability of the animals to maintain balance while walking on beams with increasing degrees of difficulty (smaller diameter, round vs square). Before injury, all of the animals could cross the three differently shaped beams without any balancing difficulties (6 points) (Fig. 9B). Seven days after the injury, the average narrow-beam score of the injured rats was severely reduced from 6 to 0.32 ± 0.02 points, indicating that most rats lost balance as soon as they were placed on the beams. After two weeks of hUCB transplantation, treated rats showed an average score of 1.71 ± 0.15, reflecting their ability to cross the whole length of the broadest beam. Over the next 3 weeks, the performance in this test recovered modestly, so that 5 weeks after the hUCB grafting, the average narrow-beam score of the injured group was 1.23 ± 0.07 and that of the hUCB-treated was 3.25 ± 0.11. The cyclosporine treated group showed a mean score of 1.3 ± 0.12. Statistically, hUCB treatment led to a significant improvement 14 d after transplantation ($p < 0.05$), which consistently increased during the whole testing period when compared with the injured group.

Contact placing response

The contact placing response was assessed in both injured and treated animals. As compared to their baseline values (mean number of responses: 7.07 per 10 trials), the animals showed a postoperative reduction in their placing response to a mean of 2.15 per hindlimb (Fig. 9C). After five weeks of SCI, injured animals showed a response of 5.97, whereas hUCB treated animals showed response up to 8.89 per 10 trails. Cyclosporine treated rats showed a response slightly better than injured animals with a score of 6.35. Interestingly, three hUCB-treated animals showed an enhanced placing response, indicating a facilitated reflex.

Discussion

Stem cell therapy, involving the introduction of healthy stem cells to repair and replace damaged or lost cells, provides much promise for the treatment of SCI. Our

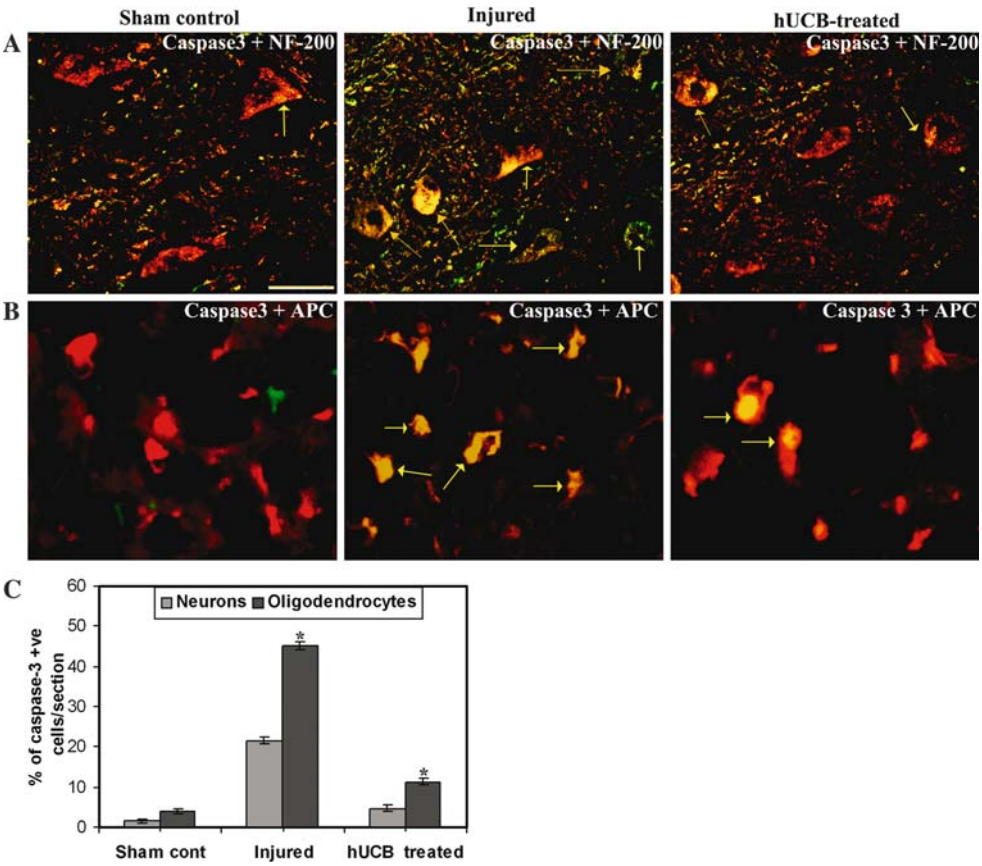

Fig. 6 Immunofluorescence analysis of caspase-3 expression in neurons and oligodendrocytes. Confocal images of cryo-sections illustrate co-localization (yellow) of activated caspase-3 (FITC-conjugated) with (**A**) NF-200 (Texas-red conjugated) and (**B**) APC (Texas-red conjugated) within the dorsal region(↑), following spinal cord contusion. The tissue sections represent regions between 1 and 2 mm caudal from the lesion epicenter after 3 weeks SCI. Bar = 100 μm. (**C**) Quantitation of apoptotic neurons and oligodendrocytes in tissue sections. A large number of caspase-3 positive cells are present in the injured sections, whereas the hUCB-treated sections exhibit a decreasing trend of caspase-3 positive cells. Values represent mean ± SEM values of at least 3 sections with duplicates between 1 and 2 mm from the injury epicenter. * Significant at $p < 0.05$, ($n \geq 4$)

results show that hUCB can be trans-differentiated to neural phenotypes in the neurogenic medium that induces differentiation of a mixed culture of neuronal population, resulting in trans-differentiation of hUCB to neurons and oligodendrocytes both under *in vitro* and *in vivo* in the injured spinal cord. These findings are consistent with the previous results (31–35) reporting that stem cells could migrate and accumulate in the injured areas, differentiate into neural cells, and improve the functional recovery of these animals.

Spinal cord trauma leads to increased expression of death receptors and their ligands as well as activation of caspases and calpain (19, 23, 36). Previous studies have shown that SCI triggers apoptotic cell death of oligodendrocytes associated with white matter tracts within 3 to 4 days after injury (20). Crowe et al., (5) reported that after SCI in the rat, typical post-traumatic necrosis occurs, but in addition, apoptotic cells were found from 6 hours to 3 weeks after injury, especially in the spinal white matter. Our results established that apoptosis follows a similar temporal profile in rats after SCI. Fas signaling has been implicated in death of motor neurons after spinal cord ischemia (37–39). Hence, inhibition of Fas may find a role in the treatment of neuronal degeneration. In the present study in SCI rats, Fas expression has been detected in both oligodendrocytes and neurons after SCI which is consistent with the earlier reports (23, 40). Our findings implicate the Fas death receptor pathway in apoptotic secondary mechanisms after SCI particularly in neurons and oligodendrocytes. Fas immunoreactivity in the white matter of the caudal segments of injured rats was higher than those of the hUCB-treated rats. Thus, hUCB downregulated Fas thereby reducing post-traumatic apoptosis in the spinal cord. These finding supports previous data showing that Fas deficiency reduces apoptosis after SCI (12). The effect of downregulation of Fas in preserving mostly oligodendrocytes is consistent with the observation that post-traumatic apoptosis in the spinal cord occurs largely in oligodendrocytes (5, 6, 14, 23, 41). Demjen et al. used FasL inhibiting antibodies to show improved neurological outcome and evidence of improved sprouting of corticospinal tract axons (24). These studies also demonstrated evidence of oligodendrocyte preservation with FasL neutralization. Inhibition of signal transduction by manipulation of molecules such as FADD and FLICE (caspase 8) inhibitory protein (FLIP) has not yet been explored. In the present investigation, hUCB appear to show the neuroprotective effects that are necessary to attenuate apoptotic processes by downregulating Fas and other extrinsic pathway proteins during secondary damage of SCI. Decreased

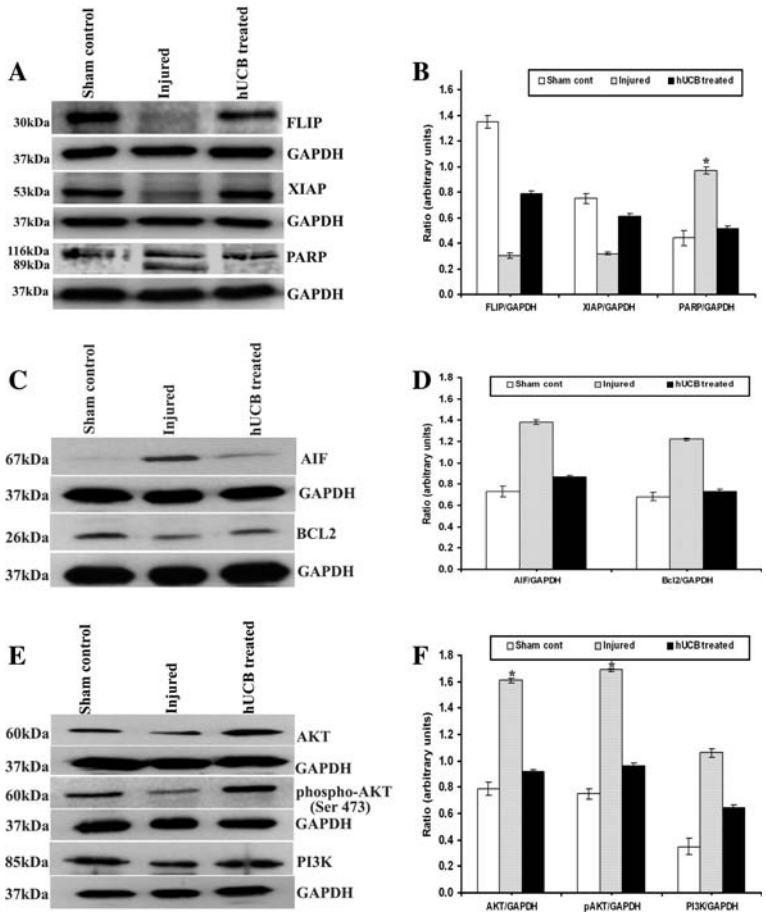

Fig. 7 Immunoblot analysis of activated inhibitors of apoptosis in spinal cord sections. Equal amounts of protein (40 μg) were loaded onto 10%–14% gels and transferred onto nylon membranes, which were then probed with respective antibodies. The blots were stripped and reprobed with GAPDH to assess protein levels. **A** and **C** shows the inhibitors of apoptosis present in cytosol and nucleus whereas **E** shows the survival signaling pathway proteins with respect to GAPDH; **B**, **D** and **F** are their quantitative estimations, respectively. Upregulation of inhibitory proteins FLIP, XIAP, and inhibition of PARP cleavage is clearly seen hUCB treatments. Each blot is representative of experiments performed in duplicate with each sample (n ≥ 3). Error bars indicate SEM. * Significant at $p < 0.05$

apoptosis in hUCB treatments was evidenced by TUNEL, caspase-3 activation assays and immuno blot analysis. Activated caspase-3 enzyme contributes to the execution of apoptosis via PARP. The present study provides the evidence that an up-regulation of PARP plays an important role in the execution of apoptosis in the injured spinal cord. Compared with injured group animals, the tissues in hUCB-treated animals had prominent decrease in breakdown of PARP protein and increase in the expression of FLIP and XIAP, which are the inhibitory proteins of apoptosis. The anti-caspase-3 activity of hUCB is attributable to downregulation of Fas and other apoptotic proteins of the extrinsic pathway, which altered the number of caspase-3-positive cells. These results strongly support that Fas triggered caspase-3 mediated apoptotic pathway is downregulated by hUCB in the cytosol as well as in the nucleus. The neuroprotective effects of hUCB are facilitated by phosphorylation of Akt at Ser 473 resulting in the activation of survival signaling pathway. However, still it is unknown as to how Fas is regulated at the membrane by hUCB.

The morphologic stability and plasticity of neuronal processes depend on the integrity of the neuronal cytoskeleton and its components (*i.e.*, actin filaments, neurofilaments, microtubules and their associated proteins) (42). MAP2 is currently considered a reliable marker of structural integrity as it is involved in the morphologic stabilization of dendritic processes. It modulates growth, differentiation and plasticity of neurons with key roles in neuronal responses to growth factors, neurotransmitters, synaptic activity and neurotoxins (43). Neurofilaments are key structural components of white matter axons and represent a very important group of structural proteins, which support the architecture of peripheral and central axons (44). Decreased degradation of NF200, α-tubulin and MAP2 associated with hUCB treatment provide evidence of improved structural integrity of the axons and neurons in the vicinity of the injury. Schumacher et al. reported that pretreatment with calpain inhibitor CEP-4143 inhibits calpain I activation and cytoskeletal degradation, which improved neurological function and enhanced axonal survival after traumatic SCI (45). In this study, downregulation of Fas receptor and caspase-3-mediated apoptosis results in improved neurological recovery after SCI, with improved axonal survival and preservation of cytoskeletal proteins. These results provide evidence that, these treatments to decrease delayed glial and neuronal cell death after SCI may be associated with axonal preservation. Our

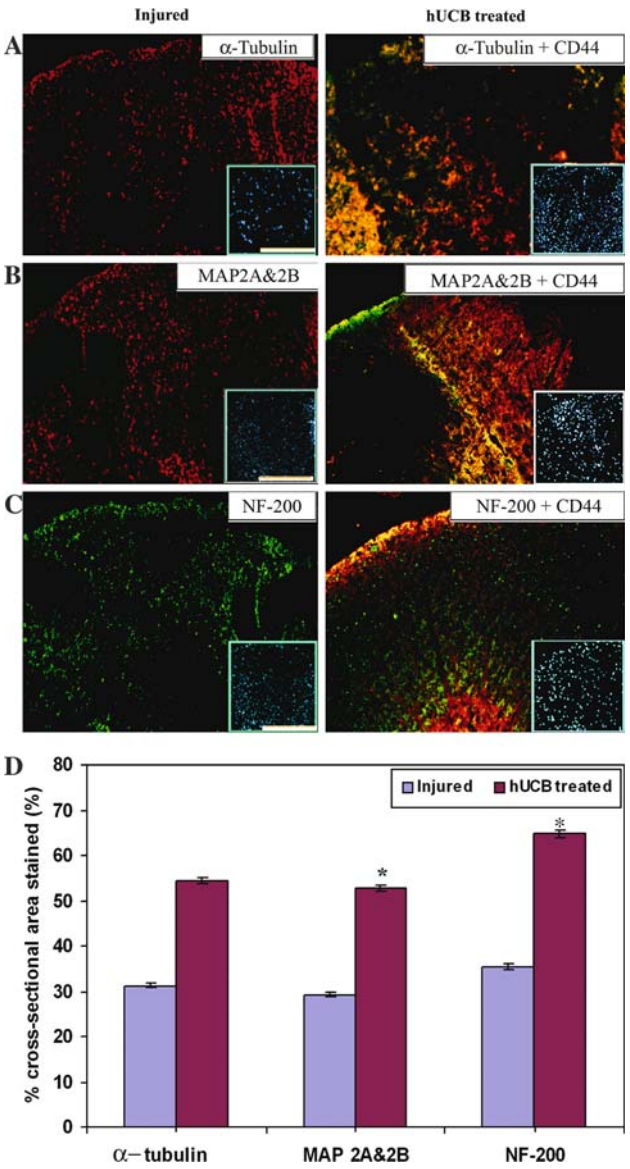

Fig. 8 Structural integrity of the injured spinal cord maintained by hUCB after intraspinal grafting. Immunofluorescence studies of spinal cord cryo-sections showing dorsal white matter with cytoskeletal markers *viz.*, α-tubulin (**A**), MAP2A & 2B (**B**) and NF200 (**C**) were performed. α-tubulin, MAP2A & 2B are Texas-red conjugated and their respective CD44 are FITC-conjugated. NF-200 is FITC-conjugated and CD44 are Texas-red conjugated. Inset shows corresponding DAPI images. Bar = 2000 μm. (**D**) Quantitative estimation of the cross-sectional area stained. Calculation of % staining was done on only the lineage specific markers, (but not on the merged image) so that exact comparison with left panel images can be done. When compared to the injured sections, hUCB-treated sections have a high level of structural integrity of the spinal cord. Values represent mean ± SEM values of at least three sections with duplicates from each condition. * Significant at $p < 0.05$. Results are from 3 independent sections between 1 and 2 mm from the injury epicenter after 3 weeks SCI (n ≥ 3)

findings implicate the role of hUCB in maintaining the structural integrity, and thereby promoting the long-term survival of neurons and oligodendrocytes.

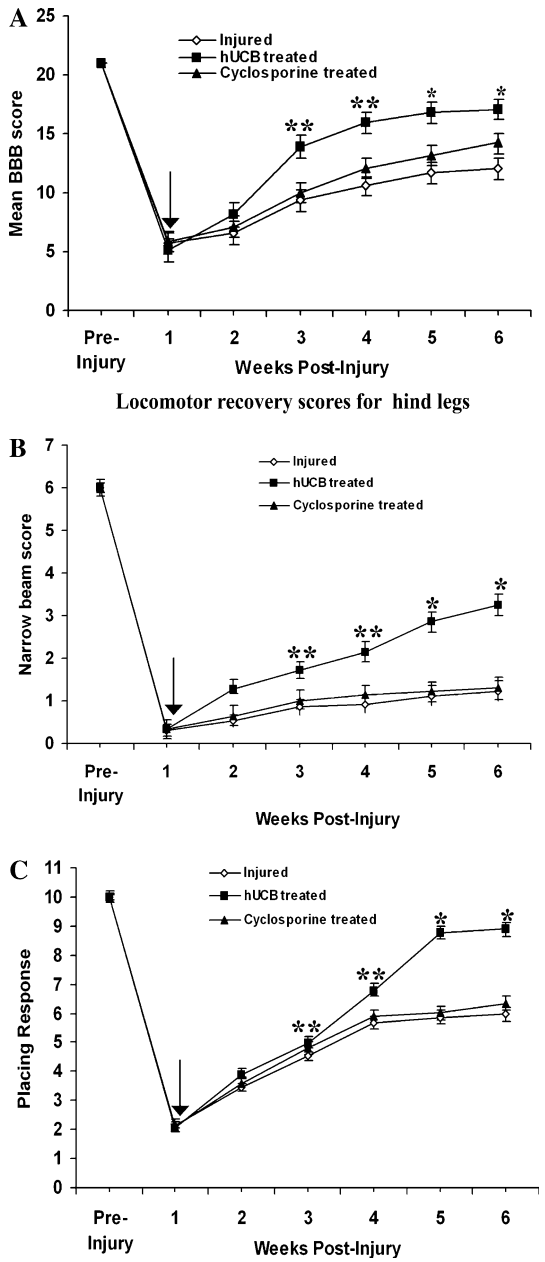

Fig. 9 Functional recovery of rats after hUCB-transplantation. (**A**) BBB scores of rats with SCI before and after hUCB transplantation. Repeated-measures of ANOVA followed by Bonferroni's post hoc tests showed that BBB scores in hUCB-grafted animals were significantly higher than those in injured-untreated animals. Each point represents the highest locomotor score achieved each day. (**B**) Narrow beam scores of injured and treated rats over a period of 6 weeks and (**C**) Number of placing responses of injured and treated animals. Arrow (↓) indicates transplantation point. Error bars indicate ±SEM (n ≥ 5 per group) (*$p < 0.01$ and **$p < 0.05$)

We found evidence of enhanced neuronal and oligodendrocyte preservation in hUCB-treated rats. There was a significant effect of hUCB in increasing the number of surviving neurons and oligodendrocytes at two weeks after grafting. Oligodendrocyte apoptosis is a widely dispersed

phenomenon during SCI that leads to long-term and persistent demyelination. As each oligodendrocyte myelinates multiple axons, their death leads to the demyelination of many fibers that are left intact by the initial trauma. The dual functions of cell death protection by reducing apoptosis and inducing regeneration of neurons and oligodendrocytes by hUCB might be involved in the functional recovery in SCI. The locomotor recovery of treated rats suggests that the Fas death receptor cascade provides a potential therapeutic target in the treatment of SCI. Yoshino et al. (40) also compared SCI in Fas-deficient *lpr* mice and wild type controls. Similar to our study, they demonstrated fewer TUNEL-positive cells, improved behavioral outcome, and a decrease in the histological evidence of injury in mutant mice.

Our study provides strong evidence that transplantation of hUCB is an effective strategy to down regulate Fas activated apoptotic mechanisms and to promote structural integration of the injured spinal cord. Our results showing robust differentiation of hUCB forming oligodendrocytes and neurons as well as improved functional neurological recovery strongly demonstrate the feasibility and efficacy of the hUCB as a potential therapeutic intervention for SCI. However, reducing apoptosis alone may not necessarily improve recovery of function. There are several mechanisms that may account for the positive effect of these hUCB, including remyelination of axons and regeneration of neurons and oligodendrocytes. The positive outcome correlates with the ability of hUCB to reduce apoptotic cell death. Long-term studies on positive effects of hUCB will provide further evidence regarding the therapeutic potential of hUCB after SCI.

Acknowledgements This research was supported by National Cancer Institute Grant CA 75557, CA 92393, CA 95058, CA 116708, N.I.N.D.S. NS47699 and NS57529, and Caterpillar, Inc., OSF Saint Francis, Inc., Peoria, IL (to J.S.R.). We thank Noorjehan Ali for technical assistance. We thank Shellee Abraham for manuscript preparation and Diana Meister and Sushma Jasti for manuscript review.

References

1. McEwen ML, Springer JE (2005) A mapping study of caspase-3 activation following acute spinal cord contusion in rats. J Histochem Cytochem 53:809–819
2. Ramer LM, Ramer MS, Steeves JD (2005) Setting the stage for functional repair of spinal cord injuries: a cast of thousands. Spinal Cord 43:134–161
3. Cohen GM (1997) Caspases: the executioners of apoptosis. Biochem J 326:1–16
4. Wallach D, Varfolomeev EE, Malinin NL, Goltsev YV, Kovalenko AV, Boldin MP (1999) Tumor necrosis factor receptor and Fas signaling mechanisms. Annu Rev Immunol 17:331–367
5. Crowe MJ, Bresnahan JC, Shuman SL, Masters JN, Beattie MS (1997) Apoptosis and delayed degeneration after spinal cord injury in rats and monkeys. Nat Med 3:73–76
6. Emery E, Aldana P, Bunge MB, Puckett W, Srinivasan A, Keane RW, Bethea J, Levi AD (1998) Apoptosis after traumatic human spinal cord injury. J Neurosurg 89:911–920
7. Li GL, Farooque M, Holtz A, Olsson Y (1999) Apoptosis of oligodendrocytes occurs for long distances away from the primary injury after compression trauma to rat spinal cord. Acta Neuropathol (Berl) 98:473–480
8. Liu XZ, Xu XM, Hu R, Du C, Zhang SX, McDonald JW, Dong HX, Wu YJ, Fan GS, Jacquin MF, Hsu CY, Choi DW (1997) Neuronal and glial apoptosis after traumatic spinal cord injury. J Neurosci 17:5395–5406
9. Shuman SL, Bresnahan JC, Beattie MS (1997) Apoptosis of microglia and oligodendrocytes after spinal cord contusion in rats. J Neurosci Res 50:798–808
10. Abe Y, Yamamoto T, Sugiyama Y, Watanabe T, Saito N, Kayama H, Kumagai T (1999) Apoptotic cells associated with Wallerian degeneration after experimental spinal cord injury: a possible mechanism of oligodendroglial death. J Neurotrauma 16:945–952
11. Warden P, Bamber NI, Li H, Esposito A, Ahmad KA, Hsu CY, Xu XM (2001) Delayed glial cell death following wallerian degeneration in white matter tracts after spinal cord dorsal column cordotomy in adult rats. Exp Neurol 168:213–224
12. Casha S, Yu WR, Fehlings MG (2005) FAS deficiency reduces apoptosis, spares axons and improves function after spinal cord injury. Exp Neurol 196:390–400
13. Citron BA, Arnold PM, Sebastian C, Qin F, Malladi S, Ameenuddin S, Landis ME, Festoff BW (2000) Rapid upregulation of caspase-3 in rat spinal cord after injury: mRNA, protein, and cellular localization correlates with apoptotic cell death. Exp Neurol 166:213–226
14. Katoh K, Ikata T, Katoh S, Hamada Y, Nakauchi K, Sano T, Niwa M (1996) Induction and its spread of apoptosis in rat spinal cord after mechanical trauma. Neurosci Lett 216:9–12
15. Lee SM, Yune TY, Kim SJ, Park DW, Lee YK, Kim YC, Oh YJ, Markelonis GJ, Oh TH (2003) Minocycline reduces cell death and improves functional recovery after traumatic spinal cord injury in the rat. J Neurotrauma 20:1017–1027
16. Lou J, Lenke LG, Ludwig FJ, O'Brien MF (1998) Apoptosis as a mechanism of neuronal cell death following acute experimental spinal cord injury. Spinal Cord 36:683–690
17. Nottingham S, Knapp P, Springer J (2002) FK506 treatment inhibits caspase-3 activation and promotes oligodendroglial survival following traumatic spinal cord injury. Exp Neurol 177:242–251
18. Nottingham SA, Springer JE (2003) Temporal and spatial distribution of activated caspase-3 after subdural kainic acid infusions in rat spinal cord. J Comp Neurol 464:463–471
19. Springer JE, Azbill RD, Knapp PE (1999) Activation of the caspase-3 apoptotic cascade in traumatic spinal cord injury. Nat Med 5:943–946
20. Springer JE, Azbill RD, Nottingham SA, Kennedy SE (2000) Calcineurin-mediated BAD dephosphorylation activates the caspase-3 apoptotic cascade in traumatic spinal cord injury. J Neurosci 20:7246–7251
21. Yong C, Arnold PM, Zoubine MN, Citron BA, Watanabe I, Berman NE, Festoff BW (1998) Apoptosis in cellular compartments of rat spinal cord after severe contusion injury. J Neurotrauma 15:459–472
22. Zurita M, Vaquero J, Zurita I (2001) Presence and significance of CD-95 (Fas/APO1) expression after spinal cord injury. J Neurosurg 94:257–264
23. Casha S, Yu WR, Fehlings MG (2001) Oligodendroglial apoptosis occurs along degenerating axons and is associated with FAS and p75 expression following spinal cord injury in the rat. Neuroscience 103:203–218

24. Demjen D, Klussmann S, Kleber S, Zuliani C, Stieltjes B, Metzger C, Hirt UA, Walczak H, Falk W, Essig M, Edler L, Krammer PH, Martin-Villalba A. (2004) Neutralization of CD95 ligand promotes regeneration and functional recovery after spinal cord injury. Nat Med 10:389–395
25. Garbuzova-Davis S, Willing AE, Saporta S, Bickford PC, Gemma C, Chen N, Sanberg CD, Klasko SK, Borlongan CV, Sanberg PR. (2006) Novel cell therapy approaches for brain repair. Prog Brain Res 157:207–222
26. Moezzi L, Pourfathollah AA, Alimoghaddam K, Soleimani M, Ardjmand AR (2005) The effect of cryopreservation on clonogenic capacity and in vitro expansion potential of umbilical cord blood progenitor cells. Transplant Proc 37:4500–4503
27. Basso DM, Beattie MS, Bresnahan JC (1995) A sensitive and reliable locomotor rating scale for open field testing in rats. J Neurotrauma 12:1–21
28. Merkler D, Metz GA, Raineteau O, Dietz V, Schwab ME, Fouad K (2001) Locomotor recovery in spinal cord-injured rats treated with an antibody neutralizing the myelin-associated neurite growth inhibitor Nogo-A. J Neurosci 21:3665–3673
29. Kunkel-Bagden E, Dai HN, Bregman BS (1993) Methods to assess the development and recovery of locomotor function after spinal cord injury in rats. Exp Neurol 119:153–164
30. Metz GA, Merkler D, Dietz V, Schwab ME, Fouad K (2000) Efficient testing of motor function in spinal cord injured rats. Brain Res 883:165–177
31. Kuh SU, Cho YE, Yoon DH, Kim KN, Ha Y (2005) Functional recovery after human umbilical cord blood cells transplantation with brain-derived neutrophic factor into the spinal cord injured rat. Acta Neurochir (Wien) 147:985–992
32. Liu S, Qu Y, Stewart TJ, Howard MJ, Chakrabortty S, Holekamp TF, McDonald JW (2000) Embryonic stem cells differentiate into oligodendrocytes and myelinate in culture and after spinal cord transplantation. Proc Natl Acad Sci USA 97:6126–6131
33. Lu P, Jones LL, Tuszynski MH (2005) BDNF-expressing marrow stromal cells support extensive axonal growth at sites of spinal cord injury. Exp Neurol 191:344–360
34. Lu P, Jones LL, Snyder EY, Tuszynski MH (2003) Neural stem cells constitutively secrete neurotrophic factors and promote extensive host axonal growth after spinal cord injury. Exp Neurol 181:115–129
35. Saporta S, Kim JJ, Willing AE, Fu ES, Davis CD, Sanberg PR (2003) Human umbilical cord blood stem cells infusion in spinal cord injury: engraftment and beneficial influence on behavior. J Hematother Stem Cell Res 12:271–278
36. Banik NL, Matzelle D, Gantt-Wilford G, Hogan EL. (1997) Role of calpain and its inhibitors in tissue degeneration and neuroprotection in spinal cord injury. Ann NY Acad Sci 825:120–127
37. Matsushita K, Wu Y, Qiu J, Lang-Lazdunski L, Hirt L, Waeber C, Hyman BT, Yuan J, Moskowitz MA (2000) Fas receptor and neuronal cell death after spinal cord ischemia. J Neurosci 20:6879–6887
38. Sakurai M, Hayashi T, Abe K, Sadahiro M, Tabayashi K (1998) Delayed selective motor neuron death and fas antigen induction after spinal cord ischemia in rabbits. Brain Res 797:23–28
39. Ugolini G, Raoul C, Ferri A, Haenggeli C, Yamamoto Y, Salaun D, Henderson CE, Kato AC, Pettmann B, Hueber AO (2003) Fas/tumor necrosis factor receptor death signaling is required for axotomy-induced death of motoneurons *in vivo*. J Neurosci 23:8526–8531
40. Yoshino O, Matsuno H, Nakamura H, Yudoh K, Abe Y, Sawai T, Uzuki M, Yonehara S, Kimura T. (2004) The role of Fas-mediated apoptosis after traumatic spinal cord injury. Spine 29: 1394–1404
41. Li GL, Brodin G, Farooque M, Funa K, Holtz A, Wang WL, Olsson Y (1996) Apoptosis and expression of Bcl-2 after compression trauma to rat spinal cord. J Neuropathol Exp Neurol 55:280–289
42. Kolb B, Whishaw IQ (1998) Brain plasticity and behavior. Annu Rev Psychol 49:43–64
43. Johnson GV, Jope RS (1992) The role of microtubule-associated protein 2 (MAP-2) in neuronal growth, plasticity, and degeneration. J Neurosci Res 33:505–512
44. Stys PK, Jiang Q (2002) Calpain-dependent neurofilament breakdown in anoxic and ischemic rat central axons. Neurosci Lett 328:150–154
45. Schumacher PA, Siman RG, Fehlings MG (2000) Pretreatment with calpain inhibitor CEP-4143 inhibits calpain I activation and cytoskeletal degradation, improves neurological function, and enhances axonal survival after traumatic spinal cord injury. J Neurochem 74:1646–1655